# FRINGE INTERFEROMETRY IN SPACE: THE FINE STRUCTURE OF R136A WITH THE ASTROMETER FINE GUIDANCE SENSOR ABOARD HST

M.G. LATTANZI
*Space Telescope Science Institute,*
*Affiliated with the Astrophysics Division,*
*SSD, ESA; on leave from Oss. Astr. di Torino*

R. BURG
*Johns Hopkins University*

J.L. HERSHEY, L.G. TAFF AND S.T. HOLFELTZ
*Space Telescope Science Institute*

AND

B. BUCCIARELLI
*Osservatorio Astronomico di Torino*

**Abstract.**

We report on the highest angular resolution observation to date of the bright core, R136a, of the massive star cluster R136 within the 30 Doradus complex in the LMC. This visual observation was obtained with the interferometric fringe mode of operation of Fine Guidance Sensor No. 3 (FGS3) on board HST. Crowding and strong diffuse background from nebular emission make this a challenging observation.

The giant HII region 30 Dor has provided some of the best candidates for the most massive stars, like R136a1. We provide evidence for a new component, R136a1B, within the previously known R136a1-a2 system with a separation of 80 mas (or $\approx$ 4000 au from a1 at the distance of the LMC), and $\Delta V = 1.1$ mag fainter than the brightest component a1. Estimates from current evolutionary models of massive stars based on the new FGS photometry predict, after subtraction of a1B, that the present mass of R136a1 is 30 $M_\odot$ with a main sequence progenitor of 60 $M_\odot$. To date, this is the *lowest* direct estimate of the mass of R136a1.



*E. Høg and P. K. Seidelmann (eds.),*
*Astronomical and Astrophysical Objectives of Sub-Milliarcsecond Optical Astrometry,* 95–100.

The success of this difficult observation adds a new, unique feature to FGS3 and gives a much expanded, astrophysically very rewarding, role to the interferometer.

## 1. Introduction

We discuss a 10–minute TRANSfer Mode observation with FGS3, taken as part of that portion of the STScI FGS Cycle 3 Calibration program designed to explore *new* and *unique* ways of using the interferometric capabilities of this instrument. TRANS mode samples the visibility fringe (or Transfer Function, TF) produced by the Koester's prism–based interferometers inside FGS3.

The choice of the target, the core (R136a) of the massive star cluster R136 in 30 Dor, was motivated by its fundamental importance as the site of some of the most massive stars known. Indeed, the establishment of an upper mass limit for individual stars remains an open question of great importance in astronomy. Its resolution will influence the studies of stellar evolution, HII regions and galaxy evolution. In particular, R136a had for many years been unresolved and its structure and photometry are still not fully explored.

The challenges for the FGS in this never–attempted–before observation were: a) crowding (R136a has the appearance of a relatively dense open cluster), and b) the high background level from nebular emission (Burg et al. 1994).

In this paper, emphasis is on the technical details of this difficult interferometric observation and its interpretation (sections 2 and 3). Some of the astrophysical implications of the results are discussed in section 4.

## 2. The Observation

The FGS measurements consist of ten, identical position angle, consecutive "Transfer Scans", each 2."1 long with 0.8 mas step size, through R136a. As described in the FGS Instrument Handbook (Version 4.0), and in recently published papers (Bernacca, Lattanzi et al. 1993; Lattanzi et al. 1994) each scan samples the interference fringe produced by the Koester's prism interferometer, the "heart" of the Fine Guidance Sensor. The Koester's prism works with an *afocal* polarized beam. There are two Koester's prism interferometers in each FGS. These are fed by a beam–splitter (which provides the required polarization) to give sensitivity in two orthogonal directions, usually referred to as X and Y axes. When a scan is executed, the FGS 5" x 5" instantaneous field–of–view scans across the target at a fixed 45°

https://doi.org/10.1017/S0074180900227915 Published online by Cambridge University Press

angle to the X and Y axes. Therefore, each FGS3 scan produces two fringes which can then be independently analyzed for signatures other than those characteristic of the FGS3 X and Y TFs of the standard single star UP69; which is observed with the same instrument setup as for the science observation. Indeed, the deviations from the single star TFs are used to measure multiple objects (see next section).

We can regard the X (Y) scan as driving a slit of the size of the resolution limit in X (Y) and 5" wide in the Y (X) direction along the scan path. Another object appearing anywhere in the rectangular slit has the *same* projected X (Y) coordinate, within the resolution limit, as that of the primary target. The resulting fringe (given as counts from the two PMTs for the given axis, i.e. $C_A - C_B$) will have an amplitude which is the sum of the two individual fringe amplitudes.

In the configuration used, the FGS can be considered a *white light* interferometer with a central wavelength of 583 nm and a bandpass (FWHM) of 234 nm. Therefore, the fringe sampled at each scan corresponds to the Fourier transform of the "real" central fringe which would form on the focal plane of the 2.5m, filled, aperture (the HST primary mirror).

The PMT integration time per pixel during each scan was 0.025 sec. To increase the signal–to–noise ratio (S/N) the 10 scans were added together for a total exposure time of 10.3 min. Each scan has a S/N of $\simeq 3$. Co–adding the scans increased the S/N to $\sim 11$, consistent with the expected improvement of $\sqrt{10}$.

The stability of the platform, i.e. the accurate control of the telescope pointing during FGS scans through a source, is of utmost importance for the success of this kind of observations. This is addressed in the work by Bradley (1994), which shows that a pointing stability of $\approx 2$ mas residual jitter is routinely achieved.

## 3. Interferometry of Multiple Stars

The observed R136a region is almost coincident with that of the high-resolution FOC F/288 image discussed by Weigelt et al. (1991). For details on the scan orientation and the field see Lattanzi et al (1994).

The presence of several point sources in the FGS FOV during the scan with separations larger than the FGS resolution limit will generate the complex fringe in Eq.(1). There, S(X) is the *normalized* single–star TF [i.e., $(C_A - C_B)/(C_A + C_B)$, $S(X + \Delta X_i)$ is the same as S(X) but displaced along the X-axis by $\Delta X_i$, the projected separation of the i–th component from R136a1, $\Delta m_i$ is the magnitude difference between the two stars, and $nc$ is the total number of point like sources in the scan. There is an analogous expression, M(Y), for the multiple star Y–axis fringe.

https://doi.org/10.1017/S0074180900227915 Published online by Cambridge University Press

$$M(X) = \frac{S(X) + \Sigma_{i=1}^{nc}\ 10^{-0.4\Delta m_i}\ S(X + \Delta X_i)}{1 + \Sigma_{i=1}^{nc}\ 10^{-0.4\Delta m_i}} \quad (1).$$

According to Eq.(1), the presence of companion stars decreases the fringe visibility (its peak–to–peak value) of the bright star; the worst case being that of components of the same magnitude as that of the "primary" star. Because of the denominator, $C_A + C_B$, in the expression of S(X), the effect of the very high level of background in this field is also a reduction of the peak–to–peak amplitude of S(X) in Eq.(1) by a factor of ten as compared to average background. The observed fringe is represented by the solid curve in Fig.1. For reference, a typical peak–to–peak (single star in average background) is $\simeq 1.1$.

From the FGS data themselves, and using the technique described in Bernacca, Lattanzi et al (1994), the background from the nebular emission is estimated at V=15 mag arcsec$^{-2}$. This value is actually consistent with the contributions from H$\alpha$, H$\beta$, [O III] $\lambda\lambda$ 4959, 5007 emissions and the spectral response of FGS3 in the configuration used here.

## 4. Measuring a Multiple Star

Although the standard algorithms used with double stars must be modified for the multiple star case, the basic technique remains unaltered. Simply, the measurement of separations and magnitude differences of multiple component objects is performed, as for double stars, by measuring the departures of the corresponding TFs from the template TFs of our reference single star Upgren 69 in NGC 188 (Lattanzi et al 1994, and references therein).

Fig. 1 shows the result for the X–axis scan obtained via the correlation method, which synthesizes the best possible model from the template scans (i.e., those of the standard star UP69) and compares that to the observed scans via Eq.(1). The solid curve is the X–axis observed TF and the dashed line superimposed is the residual curve. The locations and relative amplitudes, proportional to the relative brightnesses, of the 'spikes' appearing on the abscissas represent the solutions of our adjustments. The dashed curve shown in the bottom part of Fig. 1 represents the result of applying our alternative deconvolution technique to the OBSERVED X–axis TF (Hershey 1992). There is quite good agreement between this independent method and the correlation solution. As expected, the deconvolved TFs generally overlay the locations and the relative amplitudes of the set of point source positions deduced from the synthetic TF method. There are also cases of two spikes too close together for the deconvolved TF to show two *resolved* peaks, as it is the case for the peak which overlays the a1 and a1B X–axis spikes (Fig. 1). In these cases the shapes of the peaks exhibit significant

https://doi.org/10.1017/S0074180900227915 Published online by Cambridge University Press

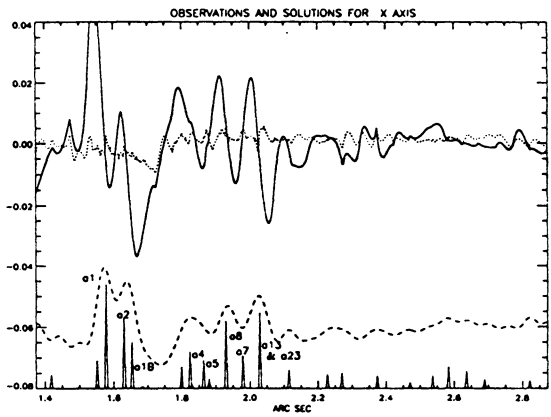


*Figure 1.* The results of interpreting the 30 Dor signal on the X axis. The thick curve is the normalized observed TF, the dotted line is the residual curve, the dashed curve is the profile generated from the deconvolution of the TF. The position and relative amplitude of the spikes on the abscissa represent the individual stellar components from our adjustments. The amplitude of the spikes is proportional to the relative brightness of the components. Only the sharpest features are identified (from Lattanzi et al 1994).

deviations from that of a fully resolved point source. Note that the projected separations and the magnitude differences are estimated at the same time. Also, the M(X) and M(Y) best–correlation fits yield two independent estimates of the $\Delta$m of each component.

The unambiguous identification of components a1, a2, and of the new component a1B from our solution is simple, since they are the closest, most luminous objects in the field. For a detailed discussion of the star identifications presented in Fig. 1 we refer to Lattanzi et al (1994). It is shown there that the FGS has "seen" all of the classical components (a1 through a8) already found by Weigelt and collaborators via speckle techniques (Weigelt and Baier 1985), plus some more previously discovered with the HST PC and FOC (pre–COSTAR) cameras.

## 5. The Case of R136a1 in The LMC

The component a1B is about $\Delta$V=1.1 mag fainter than a1 (V $\sim$ 12.75) and 80 mas away from it. The X–axis projected separation shown in Fig. 1 is $\sim$ 75 mas. Notice also that a1B is only 23 mas from a2. The estimated (internal) errors of those measurements are 0.1 mag and better than 10 mas, respectively. Ground based spectroscopy tends to classify a1 as WN6. This classification, after the subtraction of the apparent luminosity of the newly resolved component and using Maeder's models (1990), yields a present–day mass of 30 $M_\odot$ for a1 and a main–sequence progenitor of 60 $M_\odot$.

As for R136a1B, it is a very early spectral type star as well, probably an O7 V of $\sim$ 20 $M_\odot$, given the magnitude difference measured by the FGS.

https://doi.org/10.1017/S0074180900227915 Published online by Cambridge University Press

However, the luminosity class is uncertain as the FGS cannot provide any color information. It could be a much later class III giant, although this would pose a serious problem in dating the system, if one assumes that a1B is associated with the R136a complex and coeval star formation within the cluster.

## 6. Discussion and Conclusions

The results discussed in the preceding sections clearly demonstrate that the fringe mode of FGS3 is viable, in terms of both high angular resolution and accurate photometry, even in crowded fields with strong background as 30 Dor. The effect on the measurements (limiting resolution and magnitude error) of these "adverse" observing conditions appears negligible given that some of the S/N lost can be regained through the technique of co–adding consecutive scans. This new, unique, use of FGS3 gives this instrument a much expanded, astrophysically very rewarding, role.

## 7. Acknowledgements

This paper is based on observations with the NASA/ESA Hubble Space Telescope, obtained at the Space Telescope Science Institute, which is operated by the Association of Universities for Research in Astronomy, Inc., under NASA contract NAS5–26555. This work was supported in part by NASA grants NAGW–2597 and CW–0016–92. R.B. is partially supported by NASA grant NAGW–2509

We wish to thank F. Macchetto and P. Stockman for their careful reviews during the preparation of the calibration observations. We are also thankful to the members of the HST Astrometry Team (led by W. Jefferys) for stimulating discussions during their regular meetings, which affected several aspects of this work. Our warm appreciation goes to Linda Abramowicz-Reed (HDOS) for her precious help in establishing the photometric properties of FGS3 in the configuration used in this work. Finally, the useful comments of an anonymous referee are gladly acknowledged.

## References

Bernacca, P.L., et al. 1993, *A&A*, **278**, L47.
Bernacca, P.L., et al. 1994, *A&A*, in press.
Bradley, A. 1994, private communication.
Burg et al. 1994, *STScI Newsletter*, **11**, No.1,p.7).
Hershey, J.L. 1992, *PASP*, **104**, 592.
Lattanzi, M.G., et al. 1994, *ApJ*, **427**, L21.
Maeder, A. 1990, *A&AS*, **84**, 139.
Weigelt, G., and Baier, G. 1985, *A&A*, **150**, L18.
Weigelt, G. et al. 1991, *ApJ*, **378**, L22.